The Influence of Concentrated Heating on the Hadley Circulation

ARTHUR Y. HOU

Laboratory for Atmospheres, NASA Goddard Space Flight Center, Greenbelt, Maryland

RICHARD S. LINDZEN

Center for Meteorology and Physical Oceanography, Massachusetts Institute of Technology, Cambridge, Massachusetts

(Manuscript received 20 May 1991, in final form 30 September 1991)

ABSTRACT

This study extends the earlier work on Hadley circulations forced by broad, global heating distributions to situations where heating is latitudinally concentrated. In the case of heating symmetrically centered on the equator, concentration unambiguously increases the intensity of the Hadley circulation—by up to a factor of 5. For heating centered off the equator, its effect depends on whether the concentration is drawn symmetrically from both sides of the heating maximum or whether the heat is preferentially drawn from the winter side. In the latter case, concentration again leads to pronounced intensification of the Hadley circulation. Indeed, agreement between the calculated and observed Hadley intensity is achieved with mild concentration, consistent with the observed zonally averaged precipitation, rather than the narrower rainfall association with the ITCZ. This suggests that a weakening of those processes that broaden the zonally averaged rainfall (i.e., the easterly waves and regional land processes) would result in a much stronger Hadley circulation. The implication of this work is that a small change in the tropical heating distribution can profoundly alter the intensity of the Hadley circulation and the baroclinicity in the extratropics. This can, in turn, modulate wave transport in the middle and high latitudes, resulting in significant changes in the global climate.

1. Introduction

In Lindzen and Hou (1988, hereafter LH), it was shown that although Hadley circulations forced by heating off the equator were significantly stronger than those forced by heating on the equator, the calculated solstitial meridional circulations were still about 30% weaker than those derived from observations (note that in order to compare with the observed streamfunctions the calculated streamfunctions in LH must be multiplied by 2π). It was noted by LH that this discrepancy is likely not a serious one since the heating used was broad, while in reality the heat is deposited in the atmosphere in the form of latent heating, which is concentrated by low-level convergence into the narrow intertropical convergence zone (ITCZ), and more concentrated heating could readily intensify the meridional circulation. The purpose of the present paper is to explore more closely the manner in which the concentration of heating can alter the Hadley circulation.

In section 2, we examine the qualitative effects of narrow heating by means of simple "equal area" arguments of the sort developed by Held and Hou (1980), while in section 3, we discuss numerical calculations for a continuous fluid. We find that the intensity of the resulting Hadley circulation depends on how the heating is concentrated. In cases where the maximum θ_e is off the equator, the intensity of the winter circulation may be greatly enhanced if the concentration results from a redistribution over most of the winter cell. If, however, the redistribution is restricted to a width much less than that of the circulation, then the strength of the circulation does not increase significantly. The same holds true when the heating is centered on the equator.

Our results show that only a mild concentration is needed to achieve agreement with observations. Such a concentration is consistent with the observed zonally averaged concentration of rainfall (Lorenz 1967; Janowiak and Arkin 1991), rather than the much narrower local concentration associated with the intertropical convergence zone (ITCZ). Given that we are calculating a zonally symmetric circulation, this result is not surprising. It does, however, suggest that in the absence of those factors that broaden the zonally averaged concentration (i.e., easterly waves and regional variations in rainfall associated with land processes), the Hadley circulation would be much stronger. This is discussed further in section 4.

Corresponding author address: Dr. Arthur Y. Hou, NASA Goddard Space Flight Center, Laboratory for Atmospheres, Code 910.3, Greenbelt, MD 20771.

2. General considerations and "equal-area" results

It can be seen from the "equal-area" solution for an inviscid Hadley circulation (Schneider 1977; Held and Hou 1980) that concentrating the latitudinal extent of the heating leads to a stronger circulation when the forcing is symmetric about the equator; the outcome is no longer clear when heating is centered off the equator. The concentration of the heating results from the convergence of moisture in the tropical boundary layer and the ensuing localization of cumulus convection (and latent heat release in the troposphere). This low-level convergence is driven primarily by the low-level pressure gradients forced directly by the surface temperature gradients rather than by the large-scale Hadley circulation (Lindzen and Nigam 1988). Thus, moisture (and, relatedly, heat) is converged from the entire Hadley domain, including both winter and summer cells. In practice, the convergence will be mostly from the winter side of the heating maximum because of large gradients in this direction and the fact that this side includes the equator where the response to surface temperature gradients is great. We do not propose to examine this question in detail in the present paper; rather, we will analyze two extreme cases: (i) the case where the heating is concentrated symmetrically about the heating maximum and (ii) the case where the heating is concentrated unequally about the maximum heating, with most of the redistribution taking place in the winter cell. In the following sections, equal area solutions will be constructed to diagnose the extent to which concentration can alter the circulation.

a. Concentrated heating via redistribution

For the purpose of analyzing the influence of concentrated heating, the forcing function, $\theta_e(y, z)$, is perturbed in a such manner that its average over the entire Hadley domain is invariant, so that the total heat input into the system is unchanged. This is accomplished by means of a specified flux divergence on each side of the heating maximum; the resulting heating is

$$\frac{\theta_e'}{\theta_0} = \begin{cases} \theta_e(y + L_i, z)/\theta_0 + (A + \Delta_H L_i^2) \\ \quad \times \cos^2\left[\frac{\pi}{2\delta_i}(y - y_0)\right], \\ \qquad \qquad \text{for } y \text{ between } \{y_0, y_0 + \delta_i\} \\ \theta_e(y + L_i, z)/\theta_0, \\ \qquad \qquad \text{for } y \text{ between } \{y_0 + \delta_i, y_0 + L_i\} \\ \theta_e(y, z)/\theta_0, \quad \text{for } y \text{ poleward of } y_0 + L_i, \end{cases} \tag{1}$$

where the subscript i denotes "+" or "−" to differentiate quantities on the side of the summer pole from those on the winter side (see Fig. 1); $\delta_i = \frac{4}{3}\Delta_H L_i^3 (A + \Delta_H L_i^2)^{-1}$, L is the redistribution width for concentration, A is a dimensionless "perturbation amplitude" at the heating maximum; as shown in Fig. 1, and θ_e is the unperturbed heating given in LH as

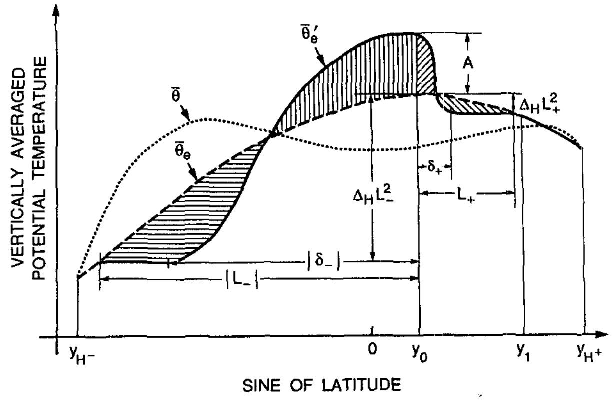

FIG. 1. A schematic showing $\bar{\theta}_e'$ as a redistribution of the unperturbed forcing, $\bar{\theta}_e$, centered at y_0. The redistribution of the applied forcing is constructed by requiring that the areas shaded with perpendicular hatches be equal. Also shown is the equal-area solution for $\bar{\theta}$ in the unperturbed case (i.e., $A = L_+ = L_- = 0$), which defines the reference Hadley boundaries, y_{H_+}, y_1, and y_{H_-}. See section 2a for details.

$$\theta_e(y, z)/\theta_0 = 1 + \frac{\Delta_H}{3}[1 - 3(y - y_0)^2] + \Delta_v\left(\frac{z}{H} - \frac{1}{2}\right)$$

in which y is the sine of latitude, z is height, H is the depth of the circulation, θ_0 is a reference potential temperature, y_0 is the position of maximum heating, Δ_H is the difference in θ_e/θ_0 from equator to pole when $y_0 = 0$, and Δ_v is the difference in θ_e/θ_0 between $z = H$ and ground.

Figure 1 illustrates the relations between $\bar{\theta}_e$, $\bar{\theta}_e'$ (where the overbar denotes the vertical average). Also shown is the equal-area solution for $\bar{\theta}$ for the unperturbed case (i.e., $A = L_+ = L_- = 0$). The equal-area solution is obtained by requiring the temperature consistent with the conservation of absolute angular momentum and the thermal wind relation to generate no net heating over the Hadley domain, which is equivalent to the conservation of θ by the Hadley circulation. The equal areas refer to the cancellation of the areas of diabatic heating and cooling (see Fig. 1 of Held and Hou 1980). The Hadley domain in the unperturbed case is shown in Fig. 1 by the poleward boundary of the summer cell, y_{H_+}, the poleward boundary of the winter cell, y_{H_-}, and the boundary between the two cells, y_1. Concentration via redistribution of the applied forcing is achieved by conserving θ_e on each side of the heating maximum at y_0; this requires that $0 \leqslant L_+ \leqslant (y_{H_+} - y_0)$, $(y_{H_-} - y_0) \leqslant L_- \leqslant 0$, and $A \geqslant A_{\min} = \max(\frac{1}{3}\Delta_H L_+^2, \frac{1}{3}\Delta_H L_-^2)$, unless $L_+ = L_- = 0$, in which case A must be zero. The condition that $A \geqslant A_{\min}$ insures $\delta_i/L_i \leqslant 1$.

The equations for the idealized Hadley circulation and the construction of the equal-area solution were described in LH. In the following sections, the parameters for the unperturbed θ_e are taken from LH to be $\theta_0 = 300$ K, $\Delta_H = 1/6$, $\Delta_v = 1/8$. The degree of concentration is thus controlled by three independent parameters: A, L_+, and L_-.

b. With the heating centered on the equator

When the heating is centered on the equator, the equal-area solution for the unperturbed θ_e gives $y_1 = y_0 = 0$, $y_{H_+} = 0.3977$ (23.43°N), and $y_{H_-} = -0.3977$ (23.43°S). Assuming a redistribution throughout the entire Hadley domain (i.e., $L_+ = y_{H_+} - y_0 = -L_- = 0.3977$), we obtain $A_{min} = 8.787 \times 10^{-3}$ (or, 2.64 K/300 K). Figure 2 displays the equal-area solutions for $A = 0$, 10/300, 20/300, 40/300, 80/300, and 160/300. As the degree of concentration increases (see Fig. 2a), Fig. 2b shows that the vertically averaged poleward heat flux (hence the meridional mass flux) increases by an order of magnitude. Note that in LH the meridional mass flux is approximated by the averaged heat flux divided by $\Delta_v\theta_0/H$. Eventually, as $A \to \infty$ ($\delta_{+/-} \to 0$), the maximum heat flux tends to a limiting value given by

$$\frac{\sqrt{1-y^2}}{\theta_0}\,\overline{v\theta}\Big|_{max} = \frac{a}{\tau}\int_{y_0+L_-}^{y_0}\frac{\bar{\theta}_e'(y_0+L_-)-\bar{\theta}(y)}{\theta_0}\,dy$$

$$= \frac{a}{\tau}\Bigg\langle -\left[1+\frac{\Delta_H}{3}-\Delta_H L_-^2-\frac{\bar{\theta}(y_1)}{\theta_0}\right]L_- + \frac{\Delta_H}{2R}\Bigg\{-\frac{1}{3}[y_0^3-(y_0+L_-)^3]+(1-2y_1^2)L_- + \frac{1}{2}(1-y_1^2)^2\left[\ln\left(\frac{1+y_0}{1-y_0}\right) - \ln\left(\frac{1+y_0+L_-}{1-y_0-L_-}\right)\right]\Bigg\}\Bigg\rangle_{y_0=y_1=0}$$

$$= -2.576\times10^{-2} \qquad (2)$$

where a is the radius of the earth, τ is the radiative relaxation time (20 days), $R = gH\Delta_H/(\Omega a)^2$, g is the gravitational acceleration, Ω is the earth's rotation rate, $\bar{\theta}_e(y_0 + L_-)/\theta_0 = 1 + \Delta_H/3 - \Delta_H L_-^2$, and $\bar{\theta}(y)/\theta_0$ is given by Eq (7) of LH.

Since $y_1 = y_0 = 0$ by symmetry, the requirement that $\bar{\theta}_e'$ and $\bar{\theta}_e$ have the same integrated value in each Hadley cell guarantees that y_{H_+} and y_{H_-} are invariant. Thus, concentration of the heating through a redistribution of heat within the Hadley domain leads to a more intense circulation without altering its meridional extent. Although the zonal wind at $z = H$ and $\bar{\theta}(y)$ produced by this inviscid circulation are not affected by redistributions of the forcing within the Hadley cell, the structure of the diabatic heating, $(\bar{\theta}_e - \bar{\theta})/\tau$, does

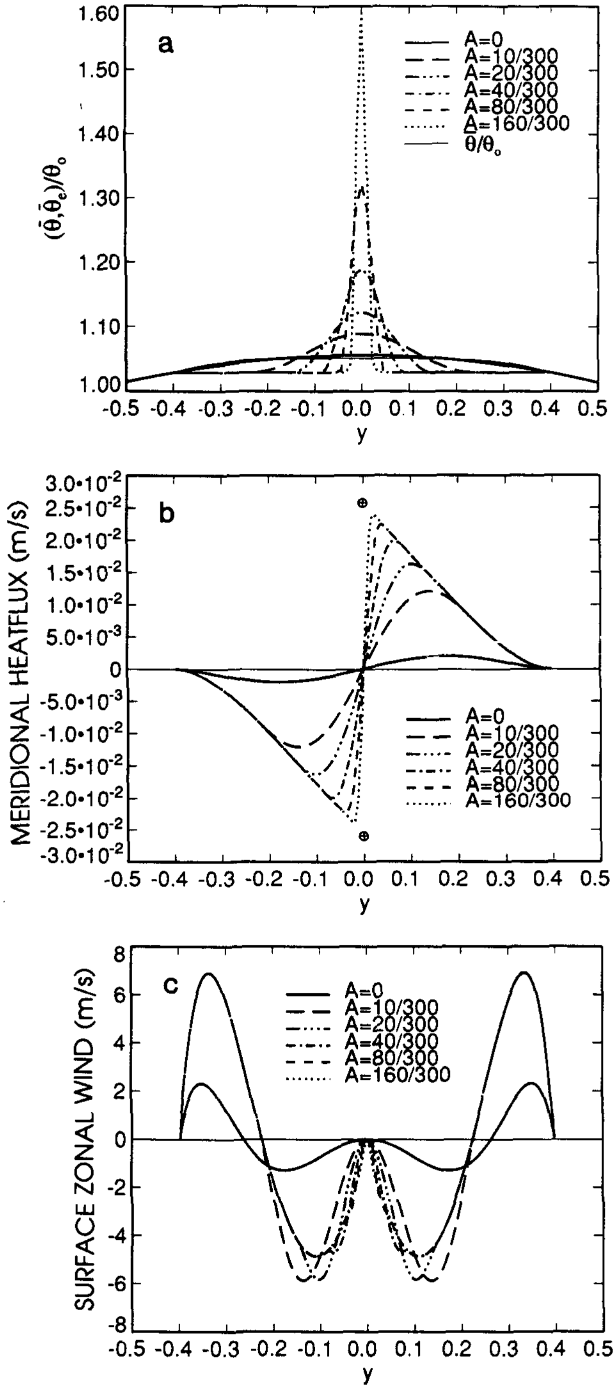

FIG. 2. Equal-area results for a heating centered at $\phi_0 = 0°$: (a) $\bar{\theta}_e/\theta_0$ (heavy lines) and $\bar{\theta}/\theta_0$ (thin line), (b) vertically averaged meridional heat flux $\theta_0^{-1}(1 - y^2)^{1/2}\,\overline{v\theta}$, with the theoretical maxima given by (2) indicated by ⊕, and (c) zonal wind at the surface. Note that both the temperature and the Hadley boundaries remain invariant as concentration increases.

reflect a narrower heating scale as the concentration increases, and the surface zonal winds also intensity (Fig. 2c).

c. *With the heating centered off the equator*

In the case where the heating is centered off the equator, the situation is more complex. For illustration, equal-area results have been obtained for $\phi_0 = 6°\text{N}$ ($y_0 = 0.10453$) and several forms of redistribution. The results are compared with that for the unperturbed θ_e, which is $\phi_1 = 20.14°\text{N}$ ($y_1 = 0.34436$), $\phi_{H_+} = 27.93°\text{N}$ ($y_{H_+} = 0.46842$), and $\phi_{H_-} = 37.33°\text{S}$ ($y_{H_-} = -0.60640$).

1) SYMMETRIC REDISTRIBUTION ABOUT THE HEATING MAXIMUM

For a symmetric redistribution within the domain of the winter cell, $y_1 - y_{H_-}$ (i.e., $L_+ = -L_- = y_1 - y_0$),

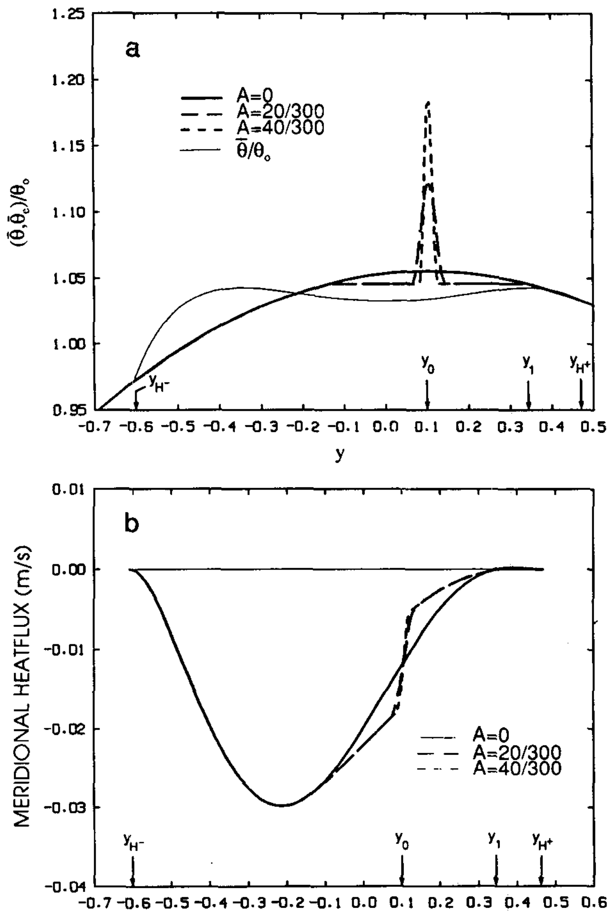

FIG. 3. Equal-area results for symmetric redistributions within the winter cell of a heating centered at $\phi_0 = 6°$: (a) $\bar\theta_e/\theta_0$ (heavy lines) and $\bar\theta/\theta_0$ (thin line) and (b) vertically averaged meriodional heat flux $\theta_0^{-1}(1-y^2)^{1/2}\,\overline{v\theta}$. Also indicated are the heating maximum, y_0, and the invariant Hadley boundaries, y_{H_+}, y_{H_-}, and y_1.

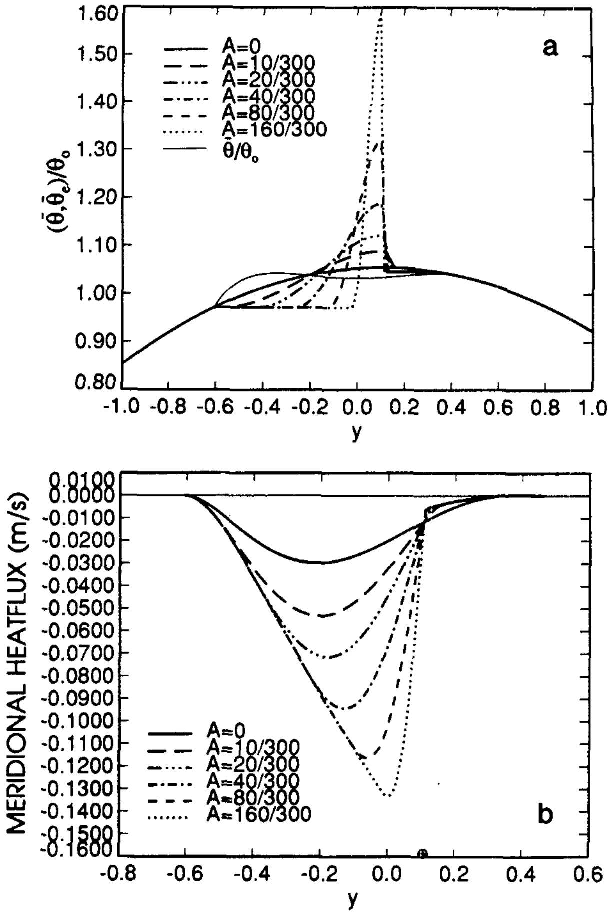

FIG. 4. Same as Fig. 3, except for asymmetric redistributions within the winter cell: (a) $\bar\theta_e/\theta_0$ (heavy lines) and $\bar\theta/\theta_0$ (thin line) and (b) vertically averaged meridional heat flux $\theta_0^{-1}(1-y^2)^{1/2}\,\overline{v\theta}$, with its theoretical maximum given by (2) indicated by ⊕.

$A_{min} = 0.96$ K/300 K. In this case, θ_e' and θ_e again have the same integrated value within each of the cells; concentration of heating does not alter the Hadley boundaries. Results for $A = 0$, 20/300, and 40/300 are shown in Fig. 3. Unlike the case where heating is centered on the equator, the heat fluxes (Fig. 3b) show practically no enhancement of the circulation. This occurs because the redistribution width, L, is significantly less than the width of the winter cell, $y_1 - y_{H_-}$ (see Fig. 3a); the result is thus a direct consequence of the assumption that the redistribution is symmetric and its width is limited by the distance between y_1 and y_0.

2) ASYMMETRIC REDISTRIBUTION WITHIN THE WINTER CELL

When the redistribution involves the entire width of the winter cell (i.e., $L_+ = y_1 - y_0$, $L_- = y_{H_-} - y_0$, $A_{min} = 8.42$ K/300 K), Fig. 4 shows that the circulation is again greatly enhanced by concentration. Figure 4b shows that the maximum averaged heat flux tends to the value of −0.1588, the theoretical limit given by (2), corresponding to an amplification by a factor of 5.

3) ASYMMETRIC REDISTRIBUTION OVER BOTH CELLS

The situation considered in the previous section is in some sense artificial since the low-level convergence is oblivious to the formal boundary distinguishing the summer and winter cells. If instead of confining the redistribution to be within the winter cell, we assume $L_+ = y_{H_+} - y_0$, $L_- = y_{H_-} - y_0$, then $\bar{\theta}_e$ and $\bar{\theta}_e'$ no longer have the same mean value in each of the cells, in which case the Hadley widths are no longer invariant. The equal-area solutions are:

$$\left.\begin{array}{ll} \phi_1' = 7.91°\text{N} & (y_1' = 0.13770) \\ \phi_{H_+}' = 22.58°\text{N} & (y_{H_+}' = 0.38402) \\ \phi_{H_-}' = 32.65°\text{S} & (y_{H_-}' = -0.53945) \end{array}\right\} \quad \text{for} \quad A = 20/300,$$

$$\left.\begin{array}{ll} \phi_1' = 6.98°\text{N} & (y_1' = 0.12155) \\ \phi_{H_+}' = 22.42°\text{N} & (y_{H_+}' = 0.38138) \\ \phi_{H_-}' = 32.47°\text{S} & (y_{H_-}' = -0.53681) \end{array}\right\} \quad \text{for} \quad A = 40/300,$$

and

$$\left.\begin{array}{ll} \phi_1' = 6.25°\text{N} & (y_1' = 0.10886) \\ \phi_{H_+}' = 22.31°\text{N} & (y_{H_+}' = 0.37962) \\ \phi_{H_-}' = 32.34°\text{S} & (y_{H_-}' = -0.53498) \end{array}\right\} \quad \text{for} \quad A = 160/300.$$

Figure 5 shows that concentrated heating again leads to a more intense winter circulation, despite an equatorward shift in the boundary between the summer and winter cells. In addition, the strength of the summer circulation is also significantly increased, although it is still much weaker than the winter cell.

The results of sections 2c(2) and (3) are intriguing in that a slight change in the heating function (namely, from one with a redistribution within the winter cell to one involving both cells) leads to a quite different solution. In this case, the boundary between the summer and winter cells shifts equatorward from 20.14°N to about 7°N, and the summer cell is appreciably stronger. It is possible, at least within the context of this idealized model, that a small change in the heating distribution could cause a rapid transition between the two solutions. But it is not clear to what extent this may be realized in the presence of waves or when the redistribution is itself affected by the circulation.

4) AN EXAMPLE OF MULTIPLE EQUAL-AREA SOLUTIONS

It should be noted that for certain θ_e profiles, there can be more than one equal-area solution. An example

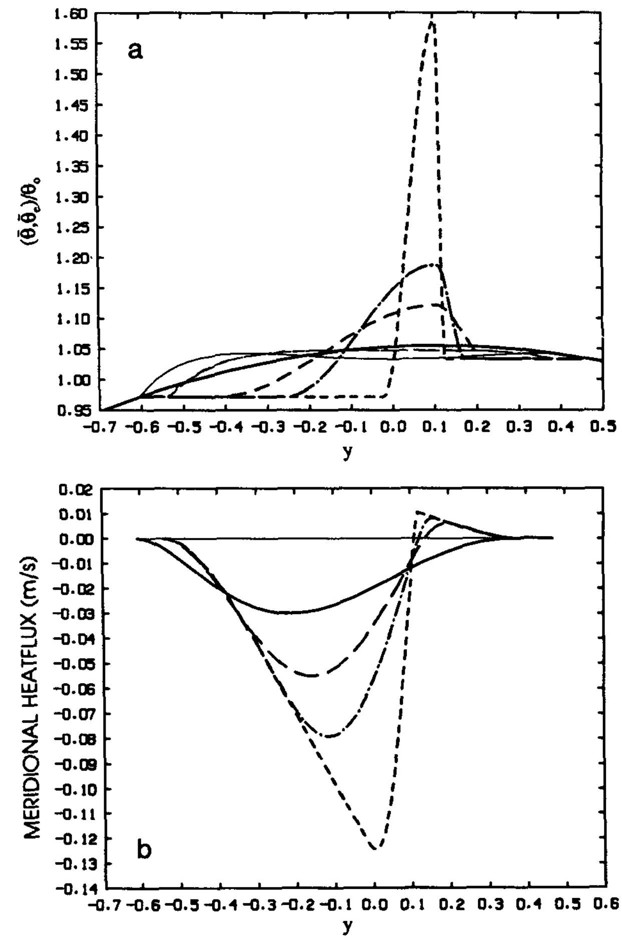

FIG. 5. As in Fig. 4 except for asymmetric redistributions over both summer and winter cells. The solid lines are for $A = 0$, the broken lines for $A = 20/300$, the dash-dots for $A = 40/300$, and the short dashes for $A = 160/300$. Here (a) $\bar{\theta}_e/\theta_0$ (heavy lines) and $\bar{\theta}/\theta_0$ (thin lines), the temperatures for the three concentrated heating cases are nearly indistinguishable from each other, and (b) vertically averaged meridional heat flux $\theta_0^{-1}(1 - y^2)^{1/2}\,\overline{v\theta}$.

is when the heating as defined by (1) is 4° off the equator ($y_0 = 0.06976$). In this case, the solution for the unperturbed θ_e is $\phi_1 = 15.85°$N ($y_1 = 0.27307$), $\phi_{H_+} = 25.74°$N ($y_{H_+} = 0.43432$), and $\phi_{H_-} = 33.23°$S ($y_{H_-} = -0.54796$).

Multiple equal-area solutions are obtained for a particular symmetric redistribution within the summer and winter cells ($L_+ = -L_- = 0.24$, $A_{min} = 0.96$ K/300 K). They are:

$$\left.\begin{array}{ll} \phi_1' = 5.18°\text{N} & (y_1' = 0.09033) \\ \phi_{H_+}' = 14.39°\text{N} & (y_{H_+}' = 0.24861) \\ \phi_{H_-}' = 27.70°\text{S} & (y_{H_-}' = -0.46487) \end{array}\right\} \quad \text{solution } S_1$$

and

$$\left.\begin{array}{ll} \phi_1' = 15.33°\text{N} & (y_1' = 0.26439) \\ \phi_{H_+}' = 24.93°\text{N} & (y_{H_+}' = 0.42146) \\ \phi_{H_-}' = 32.86°\text{S} & (y_{H_-}' = -0.54266) \end{array}\right\} \quad \text{solution } S_2.$$

The results are plotted in Fig. 6. Neither of these two solutions gives a stronger winter circulation, which is consistent with the results of section 2c (1), since the redistribution width is much less than the extent of the winter cell. Figure 6c shows that in each case the averaged diabatic heating corresponds to two thermally direct cells; in this sense both solutions are physically correct. However, the results of section 2c (3) suggest that when the redistribution involves both cells, the boundary between the two cells can shift equatorward significantly, as it does in S_1. In section 3, we will perform a numerical model experiment to verify this.

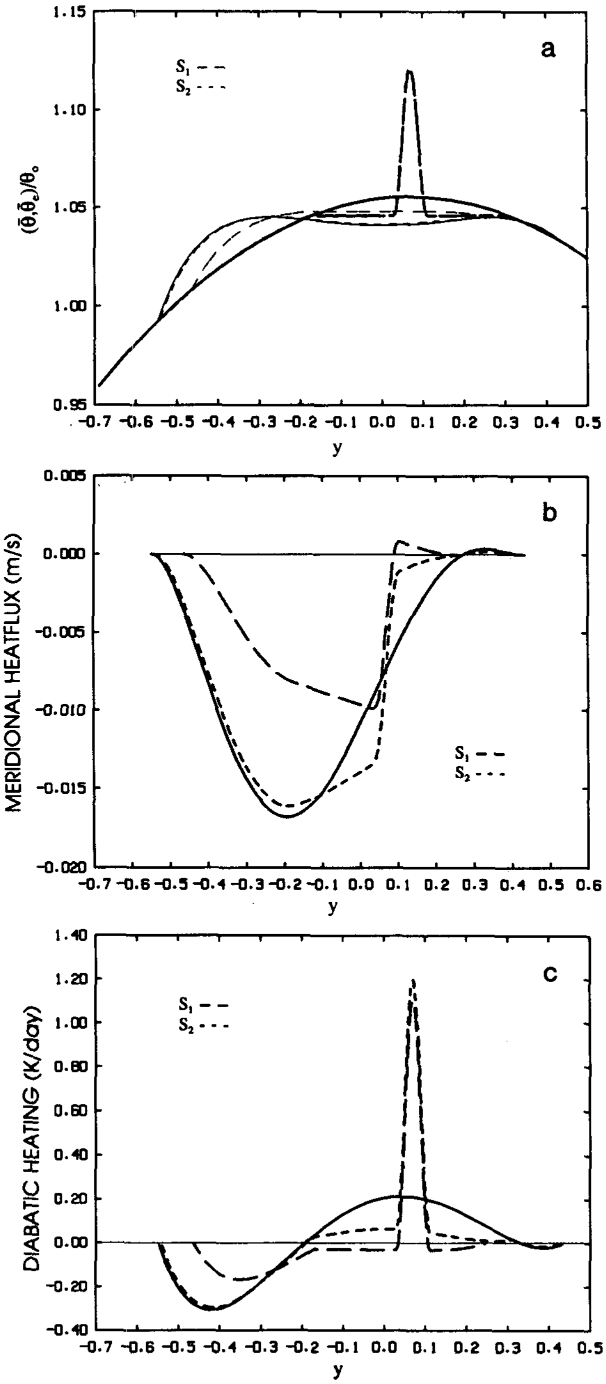

FIG. 6. Multiple equal-area solutions, S_1 and S_2 for the case discussed in section 2c (4): (a) $\bar{\theta}_e/\theta_0$ (heavy lines) and $\bar{\theta}/\theta_0$ (thin lines), the solid lines are for $A = 0$ and the broken lines for $A = 20/300$. The second equal-area solution, S_2, is given by short dashes. (b) Vertically averaged meridional heat flux $\theta_0^{-1}(1 - y^2)^{1/2}\,\overline{v\theta}$. (c) Vertically averaged diabatic heating.

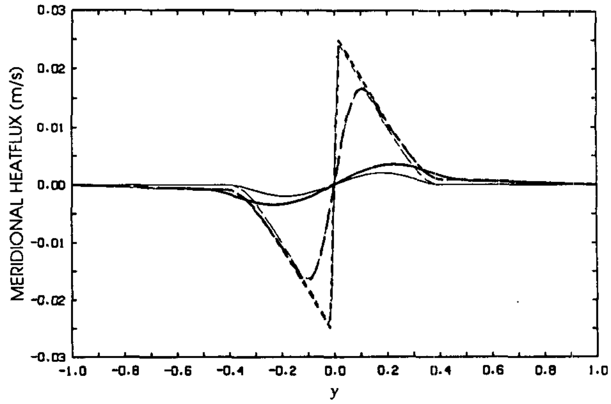

FIG. 7. Numerical model results (heavy lines) and equal-area solutions (thin lines) for the vertically averaged heat flux for $\phi_0 = 0°$. The solid lines are for $A = 0$, the broken lines for $A = 20/300$, and the dashed lines for $A = 160/300$.

3. Numerical simulations

As in LH, we verify the equal-area results using the Boussinesq numerical model of Held and Hou (1980) at a resolution of 1° latitude and 0.75 km in height. As discussed in LH, this numerical model, with its rigid lid and a highly simplified diabatic heating function, is not meant for a detailed simulation of the atmosphere. It is, however, useful for understanding the mechanics of the Hadley circulation and for testing the equal-area model. In addition to the parameters described in section 2, a vertical diffusion coefficient (ν) of 5 $m^2\,s^{-1}$ and $H = 15$ km (the same as LH) is used in our calculations. We also include a factor of 2π in the definition of the meridional streamfunction, ψ, that is,

$$v = -\frac{2\pi}{a\sqrt{1-y^2}}\frac{\partial}{\partial z}\left(\frac{\psi}{\rho_0}\right), \quad w = \frac{2\pi}{a^2}\frac{\partial}{\partial y}\left(\frac{\psi}{\rho_0}\right),$$

making it consistent with that used by Oort and Rasmussen (1970) for the observed circulation.

The excellent agreement between the equal-area solution and the numerical model result is best seen in terms of the vertically averaged heat flux. They are shown in Fig. 7 for $\phi_0 = 0°$ [cf. section 2c(1)] and in Fig. 8 for $\phi_0 = 6°$N [redistribution over both cells; cf. section 2c(3)]. The model result shows a closer agree-

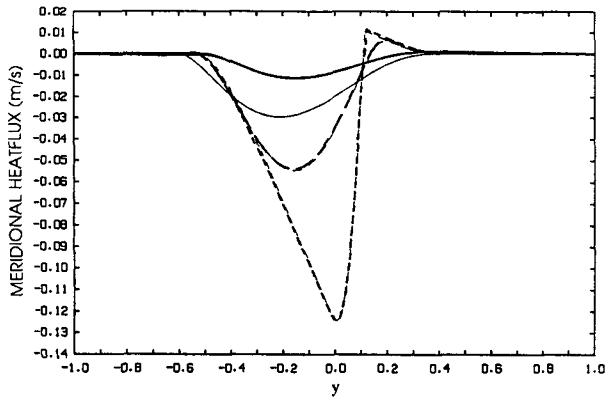

FIG. 8. Numerical model results (heavy lines) and equal-area solutions (thin lines) for the vertically averaged heat flux for $\phi_0 = 6°$. The solid lines are for $A = 0$, the broken lines for $A = 20/300$, and the dashed lines for $A = 160/300$.

ment with the equal-area solution in all cases where the heating is concentrated. The reasons are twofold: (i) Unlike the case of a broad heating, the equal-area solution for a concentrated heating predicts that ϕ_1 (the latitude at which a rising air parcel originates) is close to ϕ_0 (the latitude of maximum heating); this is precisely what happens in the numerical model—as the concentration increases, the rising motion becomes more confined to the latitude of maximum heating, bearing a closer resemblance to the idealized flow pattern. (ii) As the circulation intensifies as a result of concentrated heating, the internal viscosity in the model becomes less effective, so that the solution tends closer to the inviscid limit.

Figure 9 displays the calculated meridional streamfunctions for $\phi_0 = 6°$N. The strength of the circulation for $A = 20/300$ is nearly five times that for $A = 0$. The same amplification factor is also evident in the heat fluxes shown in Fig. 8. In this calculation, the assumed thermal forcing (i.e., the meridional gradient of θ_e) is constant with height, the resulting meridional flows are confined to boundary layers, giving rise to the double maxima in the streamfunction. If the applied heating has a maximum in the fluid interior, as in Plumb and Hou (1991), the resulting streamfunction would then have a single maximum in the midtroposphere, similar to the observed streamfunction (see Oort and Rasmussen 1970). However, the present results are adequate for demonstrating the effect of concentration

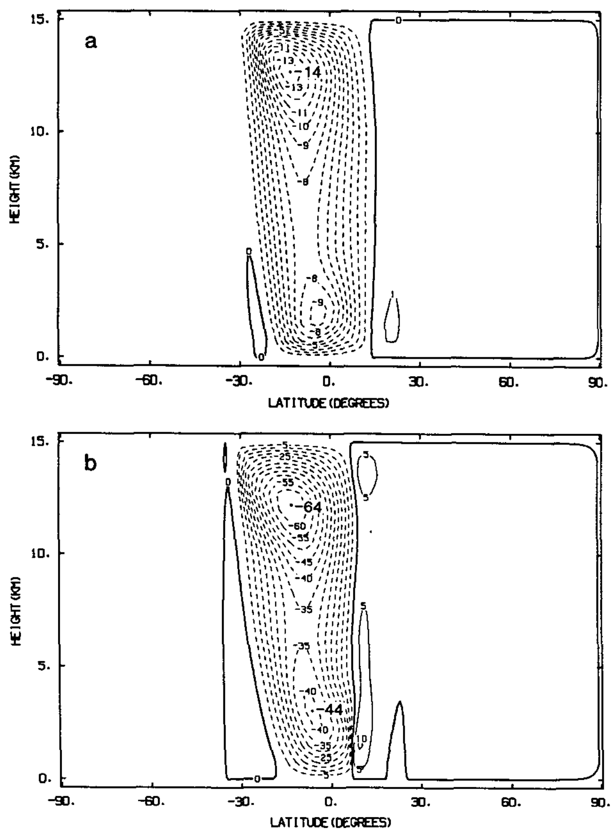

FIG. 9. Calculated meridional streamfunctions in units of 10^{10} kg s^{-1} for $\phi_0 = 6°$: (a) $A = 0$, (b) $A = 20/300$ with an asymmetric redistribution over both cells.

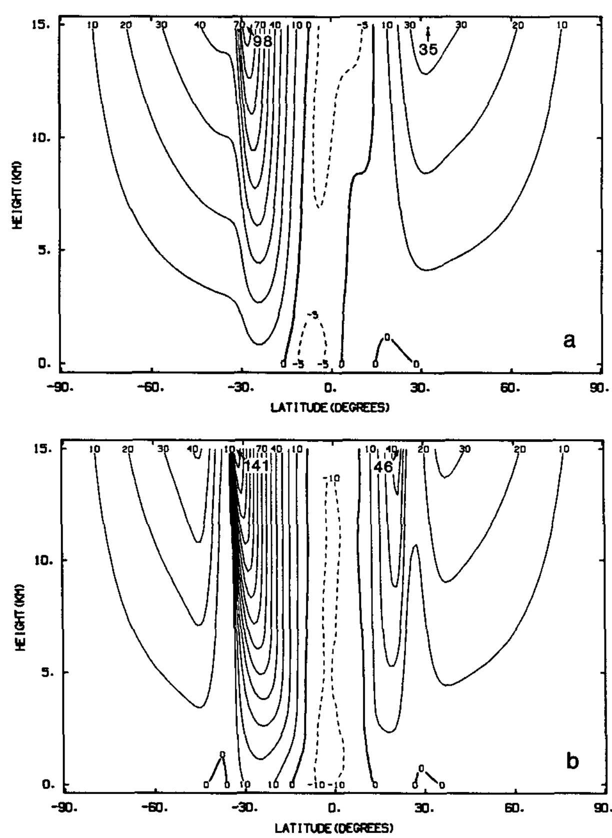

FIG. 10. Zonal winds in units of m s^{-1} for $\phi_0 = 6°$: (a) $A = 0$, (b) $A = 20/300$.

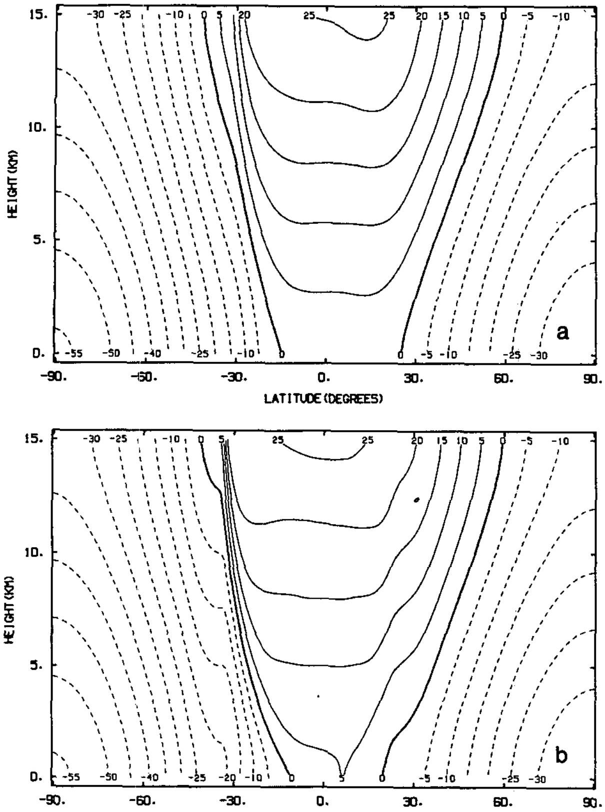

FIG. 11. Potential temperatures in kelvin for $\phi_0 = 6°$: (a) $A = 0$, (b) $A = 20/300$.

on the circulation. The observed solstitial streamfunction given by Oort and Rasmussen is typically of the order of 20×10^{10} kg s^{-1}, compared with an average of 12×10^{10} kg s^{-1} in the broad heating case (Fig. 9a). Thus, only a mild concentration is needed to achieve agreement with observations, which is consistent with the concentration of the observed zonally averaged rainfall, rather than the much narrower concentration associated with the ITCZ.

The zonal winds for the two cases are shown in Figs. 10a and 10b. The stronger meridional circulation in the presence of a concentrated heating renders the viscosity less effective, leading to a more intense winter jet and increased baroclinicity in the vicinity of the jet, which is evident in the temperatures shown in Figs. 11a and 11b. If the potential vorticity gradient is at all indicative of the intensity of baroclinic wave activities in the extratropics, Figs. 12a and 12b show that a mild concentration can, in the absence of waves, lead to a 15-fold increase in the maximum gradient and a poleward shift of its position by almost 5°. The implication is that a small change in the tropical heating structure could significantly alter wave transport at middle and high latitudes. However, this does not mean that the equilibrated subtropical jet is necessarily much stronger, but its position may be farther poleward and temperatures at high latitudes may be much warmer.

We also performed an experiment to resolve the issue concerning possible multiple solutions discussed in section 2c(4). The averaged heat fluxes shown in Fig. 13 clearly indicate that the numerical model solution corresponds to S_1 (the one in which y_1 is closer to y_0). This result is thus in accord with the conclusions of sections 2c (2) and (3).

4. Concluding remarks

We have shown that concentration in thermal forcing without changing the net energy input can greatly increase the strength of the Hadley circulation when the redistribution is over most of the Hadley domain. However, in terms of the intensity of the meridional streamfunction, only a mild concentration is needed to achieve agreement with observations. This is consistent with the observed zonally averaged concentration of rainfall, rather than the narrower concentration associated with the ITCZ. This reinforces the view that the zonally averaged circulation is primarily a response to the zonally averaged forcing. This study also suggests that in the absence of those processes that broaden the

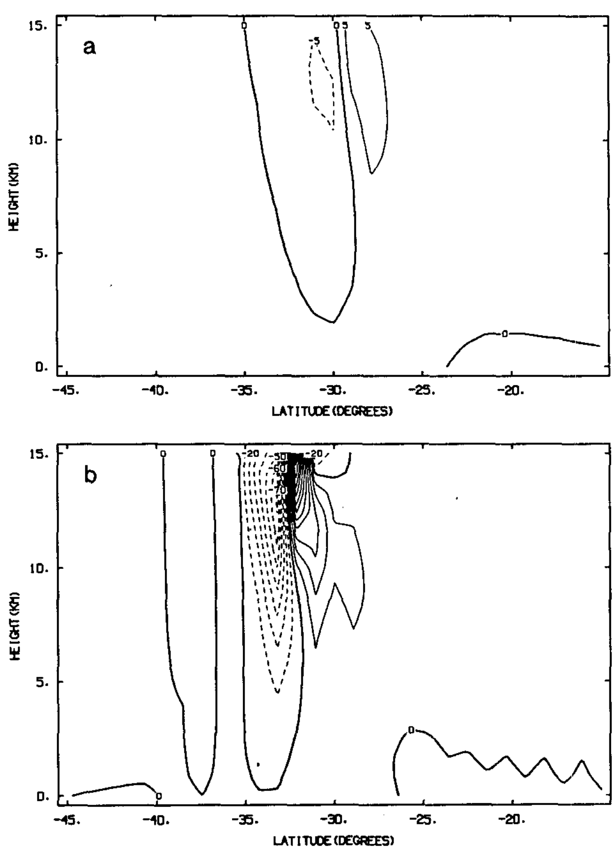

FIG. 12. Potential vorticity gradient scaled by 10^{-13} K m^2 s^{-1} for $\phi_0 = 6°$: (a) $A = 0$, (b) $A = 20/300$.

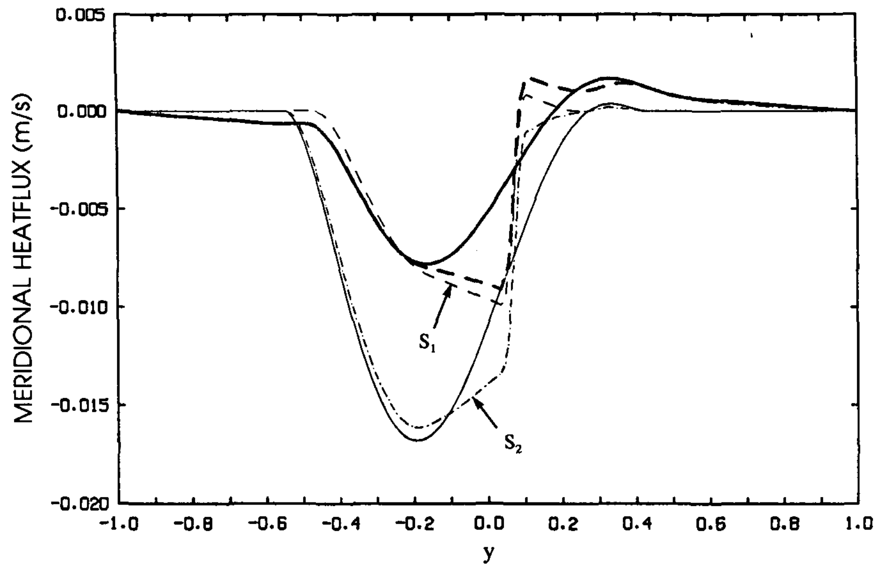

FIG. 13. Numerical model results (heavy lines) and multiple equal-area solutions (thin lines) for the vertically averaged heat flux for $\phi_0 = 4°$. The solid lines are for $A = 0$ and the broken lines for $A = 20/300$. The second equal-area solution, S_2, is marked by the dash–dot line. See text for details.

zonally averaged rainfall (e.g., easterly waves and regional variations associated with land processes), the Hadley circulation would be much stronger.

Between Lindzen and Hou (1988) and this study, we have identified two ways in which a small change in the distribution of heating (namely, displacement from the equator and concentration) can profoundly alter the intensity of the Hadley circulation and the transport of heat and momentum into the extratropics. To be sure, these diagnostic results are based on simplified zonally symmetric models without feedbacks between the forcing and the circulation. But to the extent that the behavior of the zonally averaged circulation is captured in an axisymmetric model (e.g., the sensitivity to the displacement of heating from the equator), the simple model can offer useful clues to the workings of a more complex system. In this case, the extreme sensitivity of the Hadley circulation to the latent heating distribution in the tropics raises the possibility that a small change in tropical heating could significantly alter wave transport at middle and high latitudes. Although there is as yet no direct observational evidence suggesting that variability in tropical heating distribution has an impact on the extratropical climate, this intriguing hypothesis can be readily tested in a GCM.

The various climate regimes that existed in the past were mostly characterized by changes in the pole-to-equator temperature difference rather than by changes in the mean temperature of the earth. In the present climate, there appears to be little concentration of heating, thus leaving ample scope for further increases in the Hadley intensity. If the strength of the Hadley circulation is indeed an important factor in regulating the wave transport and dynamic heating at the high latitudes, it opens the possibility that equable climates may be understood in terms of convective heating patterns that are quite different from those found in today's climate.

Acknowledgments. One of us (RSL) gratefully acknowledges the support of NSF ATM-8342482 and NASA NAGW-525, both at MIT.

REFERENCES

Held, I. M., and A. Y. Hou, 1980: Nonlinear axially symmetric circulations in a nearly inviscid atmosphere. *J. Atmos. Sci.*, **37**, 515–533.

Lorenz, E., 1967: The nature and theory of the general circulation of the atmosphere. WMO Publ. No. 218, FP. 115, 161 pp.

Janowiak, J. E., and P. A. Arkin, 1991: Rainfall variations in the tropics during 1986–89, as estimated from observations of cloud-top temperature. *J. Geophys. Res.*, TOGA/COARE Supplement, 3359–3373.

Lindzen, R. S., and A. Y. Hou, 1988: Hadley circulations for zonally averaged heating centered off the equator. *J. Atmos. Sci.*, **45**, 2417–2427.

——, and S. Nigam, 1988: On the role of sea surface temperature gradients in forcing low level winds and convergence in the tropics. *J. Atmos. Sci.*, **44**, 2440–2458.

Oort, A. H., and E. M. Rasmussen, 1970: On the annual variation of the monthly mean meridional circulation. *Mon. Wea. Rev.*, **98**, 423–442.

Plumb, R. A., and A. Y. Hou, 1991: The response of a zonally symmetric atmosphere to subtropical thermal forcing: Threshold behavior. *J. Atmos. Sci.*, in press.

Schneider, E. K., 1977: Axially symmetric steady state models of the basic state for instability and climate studies. Part II: Nonlinear calculations. *J. Atmos. Sci.*, **34**, 280–296.